Nuclear Engineering and Technology 51 (2019) 746–754

Contents lists available at ScienceDirect

Nuclear Engineering and Technology

journal homepage: www.elsevier.com/locate/net

Original Article

Determination of reaction kinetics during vitrification of radioactive liquid waste for different types of base glass

G. Suneel [a, b, *], S. Rajasekaran [b], J. Selvakumar [a, b], Chetan P. Kaushik [a, c], J.K. Gayen [b], K.V. Ravi [d]

[a] Homi Bhabha National Institute, Anushaktinagar, Mumbai, Maharashtra, 400094, India
[b] Waste Immobilization Plant, Nuclear Recycle Board, Bhabha Atomic Research Centre Facilities, Kalpakkam, Tamil Nadu, 603102, India
[c] Waste Management Division, Bhabha Atomic Research Centre, Mumbai, Maharashtra, 400085, India
[d] Nuclear Recycle Board, Bhabha Atomic Research Centre, Mumbai, Maharashtra, 400085, India

ARTICLE INFO

Article history:
Received 27 July 2018
Received in revised form
5 December 2018
Accepted 5 December 2018
Available online 8 December 2018

Keywords:
Joule melter
Cold-cap
Vitrification
Reaction kinetics
Activation energy

ABSTRACT

Vitrification of radioactive liquid waste (RLW) provides a feasible solution for isolating radionuclides from the biosphere for an extended period. In vitrification, base glass and radioactive waste are added simultaneously into the melter. Determination of heat and mass transfer rates is necessary for rational design and sizing of melter. For obtaining an assured product quality, knowledge of reaction kinetics associated with the thermal decomposition of waste constituents is essential. In this study Thermogravimetry (TG) - Differential Thermogravimetry (DTG) of eight kinds of nitrates and two oxides, which are major components of RLW, is investigated in the temperature range of 298–1273 K in the presence of base glasses of five component (5C) and seven component (7C). Studies on thermal behavior of constituents in RLW were carried out at heating rates ranging from 10 to 40 K min^{-1} using TG – DTG. Thermal behavior and related kinetic parameters of waste constituents, in the presence of 5C and 7C base glass compositions were also investigated. The activation energy, pre-exponential factor and order of the reaction for the thermal decomposition of 24% waste oxide loaded glasses were estimated using Kissinger method.

1. Introduction

Vitrification is the best available technology for fixing radioactive waste, slag content and toxic elements like arsenic into a stable and durable matrix for long term storage. Among the various host matrices available for fixing radioactive waste, borosilicate and iron phosphate glasses are globally accepted due to their durability and amenability for producing stable products [1–4]. Typically, vitrification is carried out at temperatures of 1223–1523 K, depending upon the composition of base glass and characteristics of radioactive liquid waste (RLW). The RLW generated in the closed fuel cycle contains fission products ($CsNO_3$, $Sr(NO_3)_2$ and $Ba(NO_3)_2$), corrosion products ($Fe(NO_3)_3$, Cr_2O_3, $Ni(NO_3)_2$, $Mn(NO_3)_2$ and MoO_3) and added chemicals ($NaNO_3$ and $Ca(NO_3)_2$). In the vitrification process, RLW is fed on to the top of the molten glass pool contained in an equipment called Joule Heated Ceramic Melter (JHCM). The working volume of the melter is divided into four zones and are shown in Fig. 1.

In the first zone at the top of the molten glass pool, evaporation of RLW takes place. Below this is drying zone, where moisture is removed and thermal decomposition of nitric acid occurs. In calcination zone, the dry waste constituents react with base glass beads and thermally decompose.

The products from calcination zone move into the glass-forming zone, where they turn into molten glass and get embedded into the glass structure. The first, second and third zones are collectively known as cold cap. The heat generated in molten glass by passing current between submerged electrodes is transferred through the three zones in series. The chemical reactions involved during vitrification are endothermic.

Determination of heat and mass transfer rates is necessary for rational design and sizing of a melter. In order to obtain an assured product quality, knowledge of reaction kinetics associated with the thermal decomposition of waste constituents is essential [5]. In a

* Corresponding author. Homi Bhabha National Institute, Anushaktinagar, Mumbai, Maharashtra, 400094, India.
E-mail address: suneel@igcar.gov.in (G. Suneel).

https://doi.org/10.1016/j.net.2018.12.002

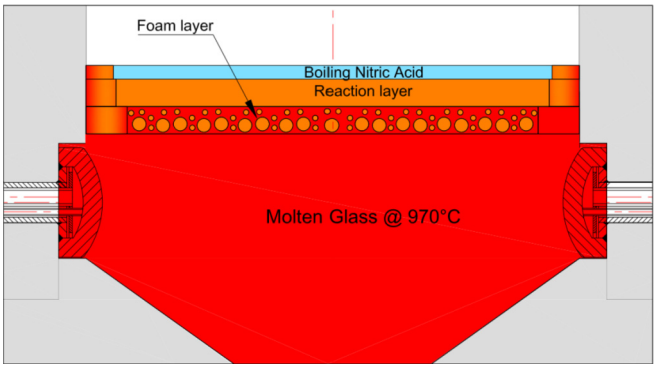

Fig. 1. Schematic of the cold cap region.

continuously fed glass melter, RLW processing rate is controlled by the rate of heat transfer from molten glass to the cold cap and by the kinetics of various chemical reactions and phase transitions within the cold cap [6].

An understanding of thermal decomposition of the waste constituents is necessary to understand the series of phenomena occurring in cold cap. Though literature pertaining to interactions of RLW constituents with base glass in cold cap region is available, not many studies investigating the effect of different glass compositions on the physicochemical reactions taking place in the cold cap are available.

Vitrification of RLW is modeled on the basis of chemical kinetics associated with all the waste constituents. For this, vitrification is mathematically expressed by system of coupled equations involving chemical kinetics, heat transfer and mass transfer. Details of the literature available on mathematical modeling of cold cap in JHCM are provided in Table 1.

As summarized in Table 1, various investigators studied the cold cap reactions of a representative waste glass feed using both simultaneous thermal analysis (STA): DSC (Differential scanning calorimetry) - Thermogravimetric analysis (TGA) and thermogravimetry coupled with gas chromatography-mass spectrometer (MS) (TGA-GC-MS) as a complementary tool for performing evolved gas analysis (EGA) [9]. The results of DSC-TGA and EGA on the cold-cap reactions provide important information for developing an advanced cold-cap model.

To determine the rate kinetics of solid state reactions, Kissinger proposed an isoconversional method based on the thermal studies (TGA or DSC) at different heating rates and this is used to determine rate kinetics during vitrification [13]. Freeman and Carroll proposed a model for thermal decomposition based on TGA to determine rate kinetics [14]. Vyazovkin et al. provided guidelines for the evaluation of kinetic parameters such as activation energy, pre-exponential factor and the reaction order from the data obtained using Thermogravimetry (TG), DSC and Differential Thermal Analysis (DTA) [15–17]. Liavitskaya and Vyazovkin analysed the reaction kinetics by an advanced isoconversional method to estimate activation energy [17].

A detailed thermo-chemical-hydraulic analysis using Computational Fluid Dynamics (CFD) for modeling melter will be a realistic approach for improving upon the prediction of glass melt rates and thus glass production rate. The model incorporating chemical kinetics could be utilized to predict the melt rate for different waste and base glass compositions and to optimize the melter operating conditions.

In the present study, thermal decomposition of waste constituents of simulated RLW (SRLW) and their thermal interactions with five component (5C) and seven component (7C) glasses under elevated temperature were investigated by TGA. Preformed glass beads were used to reduce the evaporation load of the melter and prevent foaming of glass.

The objectives of this work is to investigate the phenomena of cold cap reactions and interaction of molten glass with radioactive waste constituents and to study the influence of base glass composition on decomposition of constituents of RLW. These were addressed by carrying out TG of ten major constituents of SRLW was carried out. Activation energy, pre-exponential factor and order of the reaction for decomposition of waste nitrates and oxides in RLW to vitrified waste product (VWP) were estimated based on Thermogravimetry (TG) - Differential Thermogravimetry (DTG) analysis.

2. Experimental section

Waste constituents (equivalent of 24% waste oxide (WO) loading) were mixed with 5C and 7C glass compositions and subjected to thermal analysis. Non-isothermal weight loss measurements were carried out for the samples at different heating rates. The resulting thermogravimetric curves (change in weight versus temperature) were used to estimate activation energy (E) of the reaction by Kissinger isoconversional method. Further, the TG curves were used to predict rate constant and kinetic parameters for the thermally stimulated reactions. The investigations were carried using simultaneous thermal analyzer (Netzsch STA 449 F1 Jupiter). The dynamic TG runs of waste constituents (Table 2) were carried out at different heating rates from 10 to 40 K min^{-1} under nitogen atmosphere (100 cm^3 min^{-1}).

A pierced empty platinum crucible was used as a reference. The compositions of 5C and 7C base glasses are given in Table 2. The complete process of glass production from waste nitrates and oxides to glass melt is taking place under a non-isothermal condition in the temperature range of 323–1273 K. Table 2 also shows the

Table 1
Summary of the detailed review on cold cap modeling literature.

Investigator	Type of Waste	Kinetic Study	Contributions
Guerrero et al. [7]	Glass Slurry + SRLW	No	2D & 3D model with a simplified cold cap model that assumed the foam layer void fraction as a function of temperature. Results from laboratory batch sample testing at various temperatures were used in the study
Pokorny et al. [8]	Glass Slurry + SRLW	No	1D model for the cold cap in a slurry-fed waste glass melter was developed. Temperature and velocity fields within the cold cap were predicted.
Rodriguez et al. [9]	Glass Slurry + SRLW	Yes	TGA- DSC performed with EGA. Applied Kissinger method to estimate activation energy.
Pokorny et al. [10]	Glass Slurry + SRLW	Yes	Kinetics parameters determined by Kissinger Method and 1D model developed.
Lee et al. [11]	Glass Slurry + SRLW	No	Studied different raw materials in glass making and the effect of foam on heat flow from the molten glass to cold cap
Suneel et al. [12]	Glass Beads + SRLW	No	3D model with a simplified cold cap model from Pokorny et al. [8]

Table 2
Glass composition and simulated waste constituents.

Glass Composition			Simulated Waste Constituents (24% WO)	
Component	Weight (%)		Salt	g/L
	5C	7C	Acidity	2 N
SiO_2	48.0	54.6	$CsNO_3$	0.233
B_2O_3	26.3	11.2	$Sr(NO_3)_2$	0.081
Na_2O	11.7	14.8	$NaNO_3$	19.429
TiO_2	9.5	9.7	$Fe(NO_3)_3.9H_2O$	3.617
Fe_2O_3	4.5	2.0	Cr_2O_3	0.135
CaO	–	6.2	$Ni(NO_3)_2.6H_2O$	0.248
K_2O	–	1.5	$Mn(NO_3)_2.6H_2O$	0.740
			$Ca(NO_3)_2.4H_2O$	1.693
			MoO_3	0.135
			$BaNO_3$	0.350

composition of SRLW used in the study. These waste constituents together account for 99% of the total activity associated with RLW.

3. Kinetic model

The nth order reaction kinetics satisfactorily describes most of solid to solid and gas conversion reaction monitored by TG and Differential Thermogravimetry (DTG). In TG-DTG, the change in mass content and in thermal properties of the sample is indicated by a deflection or peak. If the reaction proceeds at a rate varying with temperature, it is evident that it possesses an activation energy. The position of the peak varies with heating rate if experimental conditions are fixed. The variation in peak temperature (T_m)

$$\alpha_i = 1 - \left[1 + \frac{(n_i - 1)A_i}{\beta}\int_0^T \exp\left(-\frac{E_i}{RT}dT\right)\right]^{1/(1-n_i)} \quad (3)$$

where β is the heating rate in K.s^{-1}

The resulting integral was exponential integral and a simple expression cannot be obtained. A satisfactory approximation is obtained using successive integration by parts after considering only first two terms in converging series of Eq. (3) by considering the weight of i^{th} reaction (w_i, fraction of mass loss in i^{th} reaction) [13].

$$\frac{d\alpha}{dT} = \frac{1}{\beta}\sum_i^p w_i A_i\left[1 + \frac{(n_i - 1)A_i}{\beta}\left(1 - \frac{2RT}{E_i}\right)\exp\left(-\frac{E_i}{RT}\right)\right]^{n_i/(1-n_i)} exp\left(-\frac{E_i}{RT}\right) \quad (4)$$

is used to determine the activation energy (E). The kinetics of reactions in solid-state are described by the equation

$$\frac{d\alpha_i}{dt} = f_i(\alpha_i)A_i exp\left(-\frac{E_i}{RT}\right) \quad (1)$$

where. $f_i(\alpha_i) = (1 - \alpha_i)^{n_i}$

α_i is the degree of conversion of i^{th} reaction, t time in seconds, A_i is the pre-exponential factor in s^{-1}, E_i is the activation energy of i^{th} reaction in J.mol^{-1}, R is the universal gas constant in J.mol^{-1}.K^{-1}, T is the temperature in Kelvin and n_i is the order of the reaction of i^{th} reaction.

Substituting $f_i(\alpha_i)$ in Eq. (1), we obtain

$$\frac{d\alpha_i}{dt} = A_i(1 - \alpha_i)^{n_i} exp\left(-\frac{E_i}{RT}\right) \quad (2)$$

In his seminal paper to determine reaction kinetics, Kissinger [13] developed a method to estimate E_i, for simple decomposition reaction regardless of reaction order by making differential thermal analysis patterns at a number of heating rates ($\beta = dT/dt$). Substituting dt with dT/β in Eq. (2). To determine degree of conversion as a function of temperature, Eq. (2) is integrated, assuming a constant heating rate. The degree of conversion of i^{th} reaction is given by following equation

In multiple reaction systems that are mutually independent in a wide temperature range ($T = T_0 + \beta t$), change of conversion with respect to temperature $\frac{d\alpha}{dT}$ is expressed interms of

$$\frac{d\alpha}{dT} = \frac{1}{\beta}\sum_i^p w_i A_i(1 - \alpha_i)^{n_i} exp\left(-\frac{E_i}{RT}\right) \quad (5)$$

where $\alpha = \sum\alpha_i$, w_i is weight of material reacted in i^{th} reaction and p indicates the major reactions.

As the temperature rises during the reaction, reaction rate $\frac{d\alpha_i}{dt}$ will rise to a maximum value, then returns to zero as shown in Fig. 3(B). If temperature rises at a constant rate, differentiating Eq. (2) with time $\frac{d^2\alpha_i}{dt^2}$ and equating it to zero provides the maximum reaction rate. Hence, by differentiating Eq. (2) and applying natural log

$$\ln\frac{E_i\beta}{RT_{im}^2} = -\frac{E_i}{RT_{im}} + \ln A_i n_i(1 - \alpha_i)^{n_i} \quad (6)$$

where T_{im} is the temperature of peak maximum in DTG curve.

According to Eq. (6), a plot between $d(ln(\beta/T^2_{im}))$ and $d(1/T_{im})$ should lead to a straight line and slope of Eq. (6)

$$\frac{E_i}{R} = -\frac{d\left(ln\left(\beta/T_{im}^2\right)\right)}{d(1/T_{im})} \tag{7}$$

where subscript m denotes the peak maximum.

Activation energy (E) is determined from a plot between $d(ln(\beta/T^2_{im}))$ and $d(1/T_{im})$ for a series of experiments at different heating rates (β).

Applying Eq. (4) for a single peak, $i = 1$

$$\frac{d\alpha}{dT} = \frac{1}{\beta} wA\left[1 + \frac{(n-1)A}{\beta}\left(1 - \frac{2RT}{E}\right)\exp\left(-\frac{E}{RT}\right)\right]^{n/(1-n)} exp\left(-\frac{E}{RT}\right) \tag{8}$$

The activation energy obtained from Eq. (7) is substituted in Eq. (8) to determine pre-exponential factor, fraction of material reacted and order of the reaction. To evaluate $\frac{d\alpha}{dT}$, all the points in TG curve are selected to cover complete reaction for each peak. The evaluated $\frac{d\alpha}{dT}$ is subtracted from experimentally obtained change of conversion with respect to temperature data. The resultant error is squared. The sum of the squares of all the errors are partially differentiated with respect to A, w & n and the resultant equations are solved simultaneously. The numerical calculations were solved using non-linear least square solver in MATLAB, 2017a software.

4. Results and discussion

The reaction mechanisms associated with conversion of melter feed to glass are complex in nature. In this study we investigated the influence of base glass composition on decomposition of constituents of RLW. Towards this purpose, TGA-DTG of ten major constituents of SRLW, preformed 5C and 7C glasses and base glasses loaded with waste constituents was carried out and presented in Fig. 2(A) and (B) and Fig. 3(A) and (B) respectively.

4.1. 5C and 7C glasses

The influence of temperature on the behavior of base glasses (5C and 7C) and their interaction with metal salts are analysed in detail. It was observed that the selected base glass matrices are stable up to 1273 K without any mass loss, which clearly indicates the promising nature of the base matrix in vitrification of RLW (Fig. 2(A)). Pure borosilicate glass (SiO_2–B_2O_3) has very low electrical conductivity. Addition of alkali oxides as modifiers to the glass formers enhances electrical conductivity and reduces the viscosity of the glass. Basically in the sodium borosilicate glass, SiO_2 and B_2O_3 form the basic glass network. Na_2O is a modifier oxide, added to achieve a fusion temperature of 1273 K, increase the electrical conductivity of molten glass and achieve a viscosity in the range of 5–10 Pa s in order to enable pouring of the molten glass in the temperature range of 1223–1273 K from the melter. TiO_2 is added to suppress Cs^{137} volatilization and Fe_2O_3 is added to improve the chemical durability and mechanical strength [18]. In 7C glass, mixed alkali elements (CaO & K_2O) are added as an additional constituents to 5C composition by lowering B_2O_3 in order to increase the concentration of the modifiers beyond their limiting concentrations. CaO and K_2O reduce the volatilization of sodium and boron possibly by satisfying the coordination number of metal ion in a better way as they have different ionic radii [19]. Hence the addition of CaO & K_2O stabilizes the glass network.

4.2. TG of SRLW constituents

In RLW, the waste constituents are present in the form of nitrates. To visualize the temperature zones for decomposition of waste constituents, the TGA studies were carried out. Thermal decomposition studies of all the waste constituents in SRLW, 5C & 7C glass loaded with 24% chemicals and 5C & 7C glass beads were performed. The mass loss with temperature and DTG curves of all the individual waste constituents are depicted in Figs. 2 and 3 respectively.

4.3. TG-DTG of fission products

$CsNO_3$ starts to decompose beyond 850 K. The first peak of DTG curve for $CsNO_3$ shown in Fig. 3(A) is decomposition of $CsNO_3$ to $CsNO_2$, which occurs between 850 K and 1023 K. Resultant $CsNO_2$ further decomposes to Cs_2O from 1023 K to 1123 K. Thermal

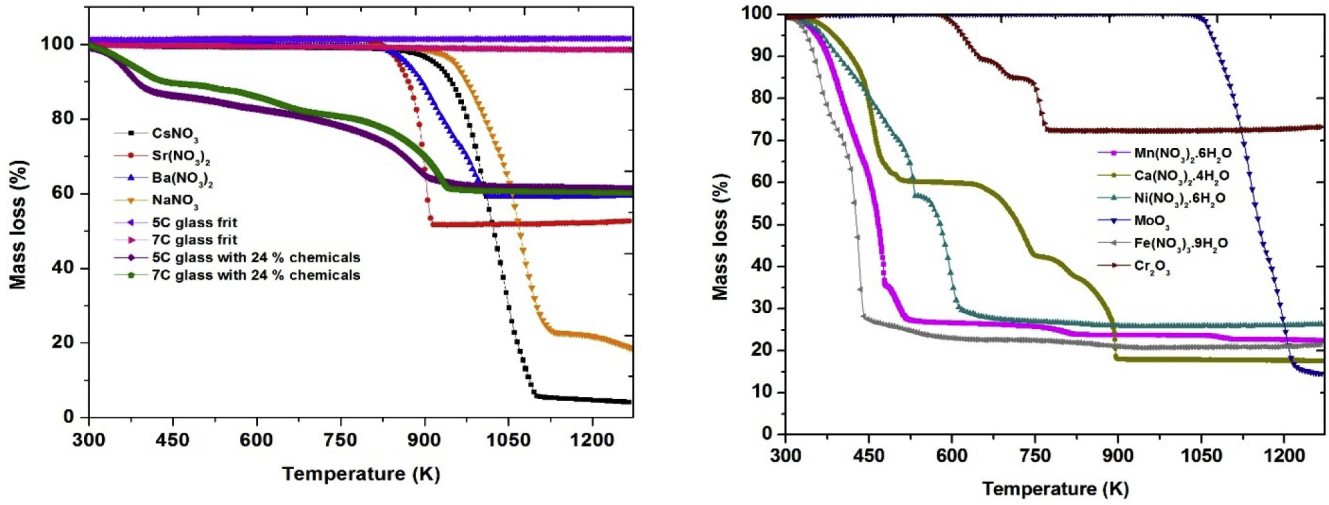

Fig. 2. (A) & (B): Mass loss with temperature of all the individual waste constituents, 5C & 7C glasses and base glass loaded with 24% chemicals using TGA for 10 K min^{-1} heating rate.

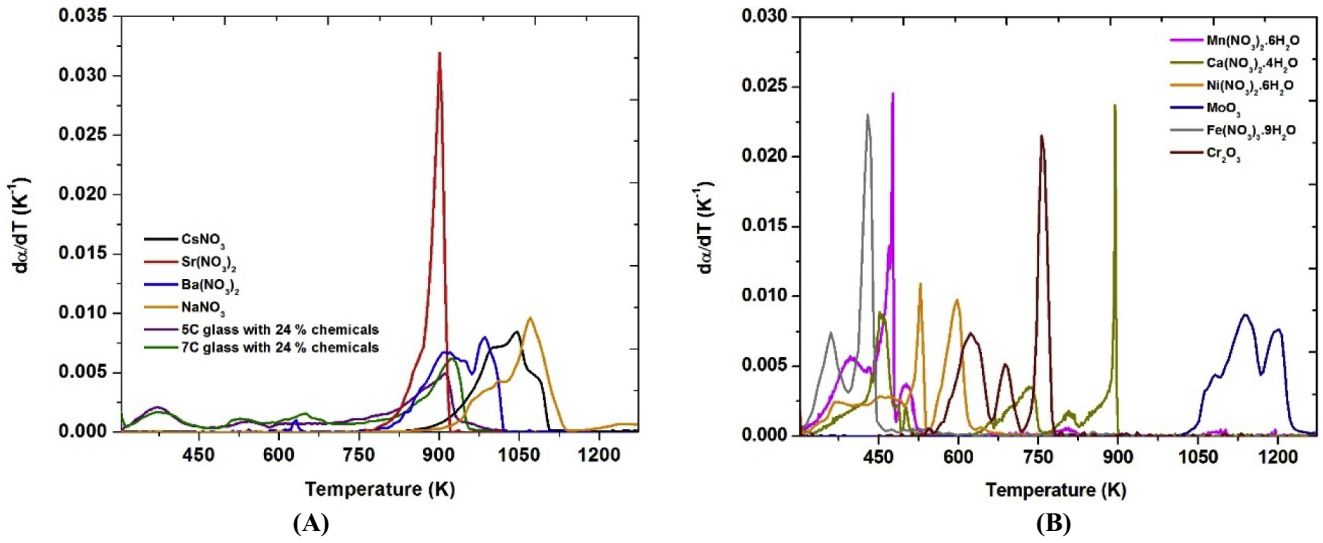

Fig. 3. (A) & (B): DTG Curves of all the individual waste constituents and 5C & 7C glass with 24% chemicals using TGA for 10 K min^{-1} heating rate.

decomposition of $Ba(NO_3)_2$ to $Ba(NO_2)_2$ takes place between 798 K and 973 K. Subsequently, it decomposes to BaO between 973 K and 1123 K. $Sr(NO_3)_2$ thermally decomposes to SrO between 773 and 923 K. The thermal decomposition pattern of $Ba(NO_3)_2$ and $Sr(NO_3)_2$ are shown in Figs. 2(A) and 3(A).

4.4. TG-DTG of corrosion products

During the thermal decomposition of ferric nitrate $Fe(NO_3)_3.9H_2O$ to Fe_2O_3, the first DTG peak in Fig. 3(B) shows dehydration of $Fe(NO_3)_2$ in the temperature range of 303 K–373 K. Subsequently, $Fe(NO_3)_2$ decomposes to Fe_2O_3 in the temperature range of 373–473 K. $Ni(NO_3)_2.6H_2O$ is decomposed to Ni_2O_3 between 473 and 540 K. Subsequently, Ni_2O_3 decomposes to NiO in range of 540–723 K. $Mn(NO_3)_2$ decomposes to MnO_2 in the temperature range of 450–850 K and it further decomposes to Mn_2O_3 between 850 and 1150 K. The thermal decomposition patterns of corrosion products are shown in Figs. 2(B) and 3(B).

4.5. TG-DTG of added chemicals

$NaNO_3$ starts to decompose beyond 900 K. The first stage of decomposition starts at 900 K and is completed at 1023 K $NaNO_3$ forms $NaNO_2$ and subsequently decomposes to Na_2O before it starts subliming above 1153 K as shown in Fig. 2(A) and (B). $Ca(NO_3)_2$ decomposes to CaO in the temperature range of 773–823 K as shown in Figs. 2(B) and 3(B). The thermal decomposition data is consolidated and presented in Table 3.

4.6. Effect of base glass composition on thermal decomposition of waste constituents

During the conversion of waste nitrates to oxides and subsequent vitrification, mass loss was observed. The mass loss curves are shown in Fig. 2(A)and (B) for individual waste constituents, 5C and 7C glasses and 5C & 7C glasses loaded with waste nitrates corresponding to 24% waste oxide.

Table 3
Thermogram of thermal decomposition

Waste Constituent	Temperature (K)								
	373	473	573	673	773	873	973	1073	1173
Fission Products									
$CsNO_3$	Sensible heating					D* to Cs_2O		$S^{\#}$	
$Sr(NO_3)_2$	Sensible heating					D to SrO			
$Ba(NO_3)_2$	Sensible heating					D to $Ba(NO_2)_2$		D to BaO	
Added Chemicals									
$NaNO_3$	Sensible heating					D to $NaNO_2$		D to Na_2O	S
$Ca(NO_3)_2.4H_2O$	$DH^{\#\#}$		Sensible heating		D to CaO		Sensible heating		
Corrosion Products									
$Ni(NO_3)_2.6H_2O$	DH		D to $Ni(NO_3)_2$		D to Ni_2O_3		Sensible heating		
MoO_3	Sensible heating						M**	D to MoO_2	
$Fe(NO_3)_3.9H_2O$	DH		D to Fe_2O_3			Sensible heating			
$Mn(NO_3)_2.6H_2O$	DH			D to MnO_2				D to Mn_2O_3	
Cr_2O_3	Sensible heating			D to CrO_x			Sensible heating		

* D – Decomposition, ** M-Melting, # S-Sublimation, ## DH-Dehydration and x=1 to 1.5

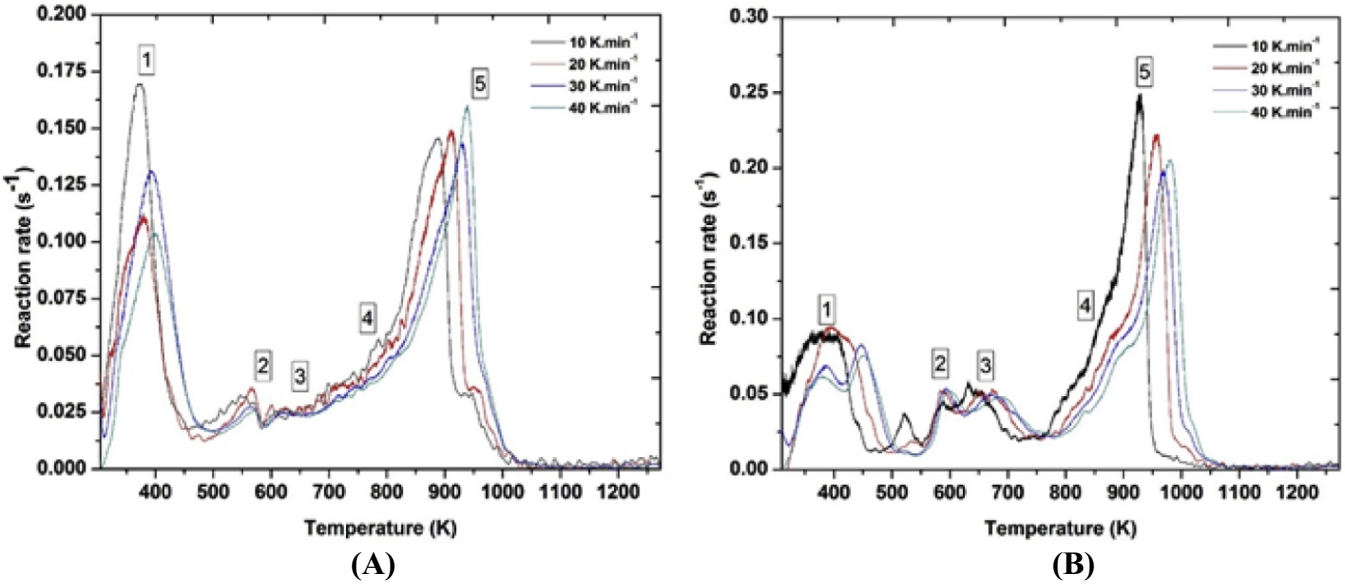

Fig. 4. DTG curves at different heating rates for (A) 5C glass (B) 7C glass.

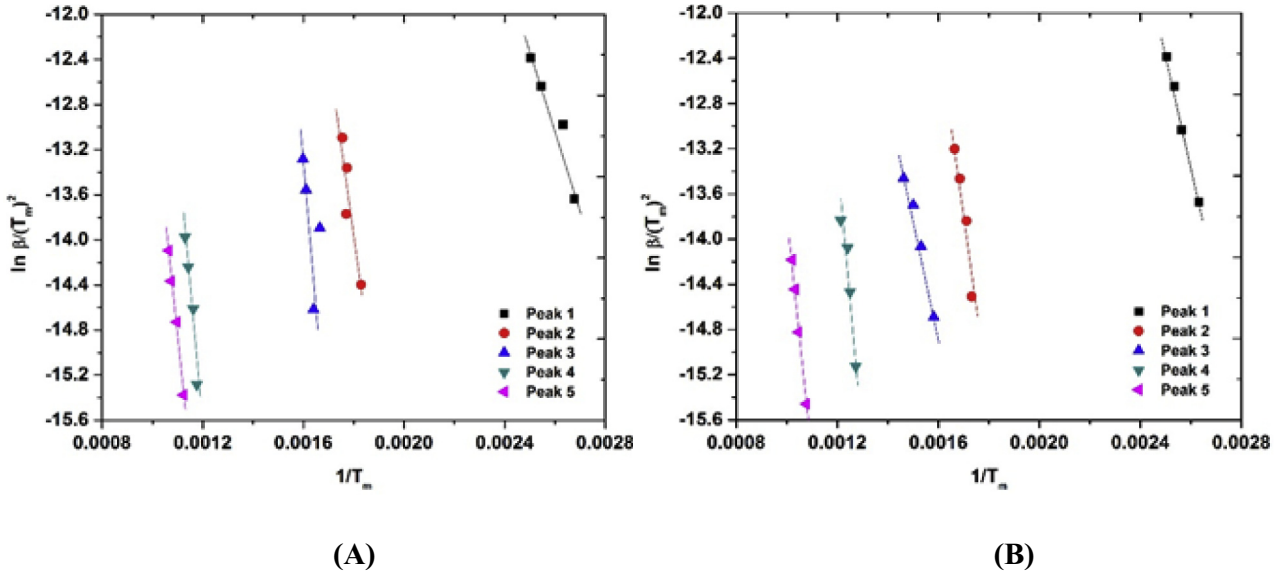

Fig. 5. Kissinger plot for (A) 5C glass & (B) 7C glass with 24% waste constituents.

Experimentally determined mass loss for 5C & 7C glasses loaded with 24% waste constituents are 34 ± 0.3% and 36 ± 0.3% respectively. 5C glass indicates lower volatile losses during vitrification compared to 7C glass. The addition of CaO in base glass increases volatility losses of waste constituents and improves glass durability [20].

7C glass loaded with waste oxides decomposes at a faster rate compared to 5C glass for peaks – 2, 3, 4 and 5 as shown in Fig. 3(A), whereas the reaction rate is lower for 7C compared to 5C for peak –1 for all the heating rates.

It was found that the thermal decomposition of $CsNO_3$ in the presence of borosilicate glasses (5C and 7C) took place at a lower temperature than that of base compound $CsNO_3$ (Fig. 3(A)). A similar phenomenon was reported by Kawai et al. [6] and Banerjee et al. [19]. Banerjee et al. inferred that an optimum level of titanium in the base glass would subdue the sublimation of Cs [19]. The decomposition reactions of the waste nitrates shift to lower temperatures in the presence of glass.

4.7. Estimation of kinetic parameters

In this study, to determine rate kinetics DTG curves for 5C and 7C base glasses with waste constituents equivalent to 24% waste oxide loading in VWP are plotted for different heating rates viz., 10 K min^{-1}, 20 K min^{-1}, 30 K min^{-1} and 40 K min^{-1} are presented in Fig. 4(A) and (B). The first three peaks in Fig. 4 represents the

Table 4
Kinetic parameters of 5C base glass during thermal decomposition.

Parameter	*logA*					*n*					*w*				
	Peak														
β (K.min^{-1})	1	**2**	3	4	5	1	2	3	4	5	1	2	3	4	5
10	6.07	10.87	7.17	9.70	8.97	2.03	1.79	1.40	2.78	1.26	0.10	0.03	0.01	0.022	0.22
20	4.18	9.47	5.44	9.80	8.47	2.04	3.36	2.69	2.61	1.10	0.08	0.02	0.02	0.004	0.21
30	6.02	11.40	7.57	7.34	8.46	2.04	2.04	2.80	1.98	1.20	0.11	0.02	0.01	0.046	0.21
40	6.08	11.35	7.78	9.30	8.35	2.04	1.73	3.37	2.52	0.81	0.09	0.02	0.01	0.046	0.21
Average	5.59	10.77	6.99	9.70	8.56	2.04	2.23	2.56	2.78	1.09	0.10	0.02	0.01	0.037	0.21
E (kJ.mol^{-1})	54.40	134.00	101.9	180.8	176.8	54.40	134.0	101.9	180.8	176.8	54.4	134.0	101.9	180.8	176.8

Table 5
Kinetic parameters of 7C base glass during thermal decomposition.

Parameter	*logA*					*n*					*w*				
	Peak														
β (K.min^{-1})	1	**2**	3	4	5	1	2	3	4	5	1	2	3	4	5
10	8.89	12.28	5.86	11.25	8.10	2.65	1.26	1.25	2.09	0.22	0.10	0.03	0.02	0.02	0.31
20	9.57	12.18	5.18	11.01	8.07	4.21	2.81	1.29	2.74	0.34	0.09	0.05	0.05	0.02	0.34
30	8.52	12.45	5.20	11.45	8.10	2.37	2.29	1.23	2.42	0.25	0.10	0.03	0.06	0.03	0.30
40	8.52	12.43	5.20	11.00	9.98	2.40	1.93	1.23	2.42	0.43	0.10	0.03	0.06	0.01	0.32
Average	8.87	12.33	5.36	11.18	8.56	2.91	2.07	1.25	2.4	0.34	0.10	0.03	0.05	0.02	0.32
E (kJ.mol^{-1})	54.40	134.00	101.90	219.61	176.80	54.40	134.00	101.90	219.61	176.80	54.40	134.00	101.90	219.61	176.80

dehydration, thermal decomposition of nitrates of corrosion products and thermal decomposition of nitrates of alkali earth metals respectively while the fourth and fifth peak depicts the thermal decomposition of the nitrates of alkali elements present in fission products and added chemicals.

In the present study, the Kissinger method [13] was applied for the determination of activation energy for major reactions. Fig. 4(A) and (B) shows the DTG curves for 5C and 7C glass at different heating rates viz., 10, 20, 30 & 40 K min^{-1}. As expected the curves shift to higher temperatures as the heating rate is increased. Also, the heights of the peaks generally decrease as the heating rates are increased as observed in peak 2, 3, 4 & 5. The shift in peaks is due to different reactions in the waste constituents. Slow-low temperature reactions are bound to get higher time during slower heating rate (10 K min^{-1}), whereas during faster heating rates (40 K min^{-1}) the conversion takes place over a temperature range due to associated lower rate kinetics. Therefore, the height of the peak reduces during faster heating rates and the starting condition of high temperature reactions are shifted towards higher temperature as shown in Fig. 4.

To apply Kissinger's method, deconvolution of DTG curves is necessary. Four major peaks were chosen as indicated in Fig. 4(A) and (B). A plot between $\left(ln\frac{\beta}{T_m^2}\right)$ and $\left(\frac{1}{T_m}\right)$ yields a straight line. The slope of the line yields the activation energy of that particular reaction. The Kissinger plots for 5C and 7C glasses loaded with waste nitrates corresponding to 24% waste oxide for all the peaks are shown in Fig. 5(A) and (B) respectively.

The activation energy obtained from the Kissinger plots facilitated the calculation of the other two important kinetic parameters i.e., pre-exponential factor and order of reaction along with fraction of weight loss. Tables 4 and 5 show the calculated values of the activation energy, pre-exponential factor, order of reaction and fraction of weight loss due to reactions happening in the peaks. Pre-exponential factor and weight of reactions are independent of rate of heating. On the other hand, order of reaction varies with heating rate by 7%, 11%, 2% and 3% for peaks 2, 3, 4 and 5 respectively for 5C and 9%, 0.3%, 0.9% and 6% for peaks 2, 3, 4 and 5 respectively for 7C when compared with average order of reaction.

Subsequently, the kinetic parameters determined in this study were substituted in the rate equation mentioned in Eq. (8) and the plots of measured and fitted values for 5C and 7C were shown in Fig. 6(A,B,C & D) and Fig. 7(A,B,C & D) respectively. Fraction of weight loss (w_i) for the desired peak was obtained from Fig. 3(A) for a particular peak. The average values of A_i, and n_i listed in Tables 4 and 5 were used to recalculate w_i and compared with experimentally determined fraction of weight loss. The total weight loss determined by fitting is 6.3% lesser compared to experimentally determined weight loss.

5. Conclusions

TG-DTG of waste constituents of RLW, was investigated from room temperature to 1273 K in the presence of base glasses of two different compositions viz., 5C and 7C glass. The study of the thermal behavior of constituents in RLW was carried out at different heating rates from 10 to 40 K min^{-1}. The TG/DTG patterns of simulated waste containing eight nitrates and two oxides were compared with patterns generated in the presence of base glass consisting of 5C and 7C compositions. The influence of base glass composition on rate kinetics was calculated. The rate of decomposition of waste nitrates to oxides is higher in 7C glass as compared to that in 5C glass.

The kinetic parameters like activation energies, pre-exponential factor and order of reaction of waste nitrates in the presence of other waste nitrates and glass constituting 5C & 7C used in the study were calculated using Kissinger's method combined with method of least-squares. Pre-exponential factor and weight of reaction are independent of rate of heating, whereas order of reaction varies with rate of heating. The kinetic parameters determined from the studies is expected to provide better understanding of the complex phenomenon in the cold cap of JHCM for vitrifying RLW.

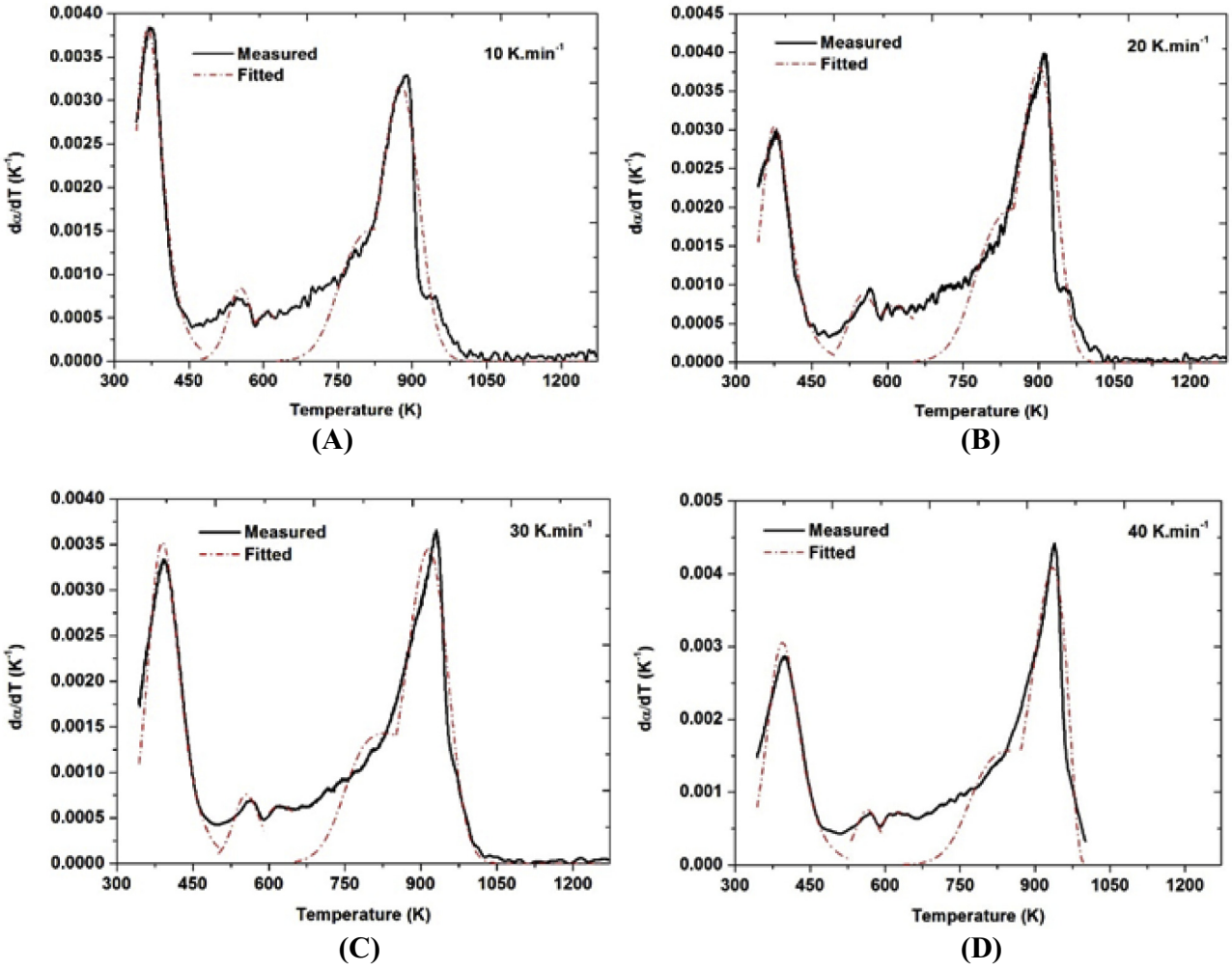

Fig. 6. Measured (solid line) and fitted (dashed line) TGA curves and deconvolution peaks for individual heating rates for 5C loaded with waste nitrates for different heating rates (A) 10 K.min^{-1}, (B) 20 K.min^{-1}, (C) 30 K.min^{-1} & (D) 40 K.min^{-1}.

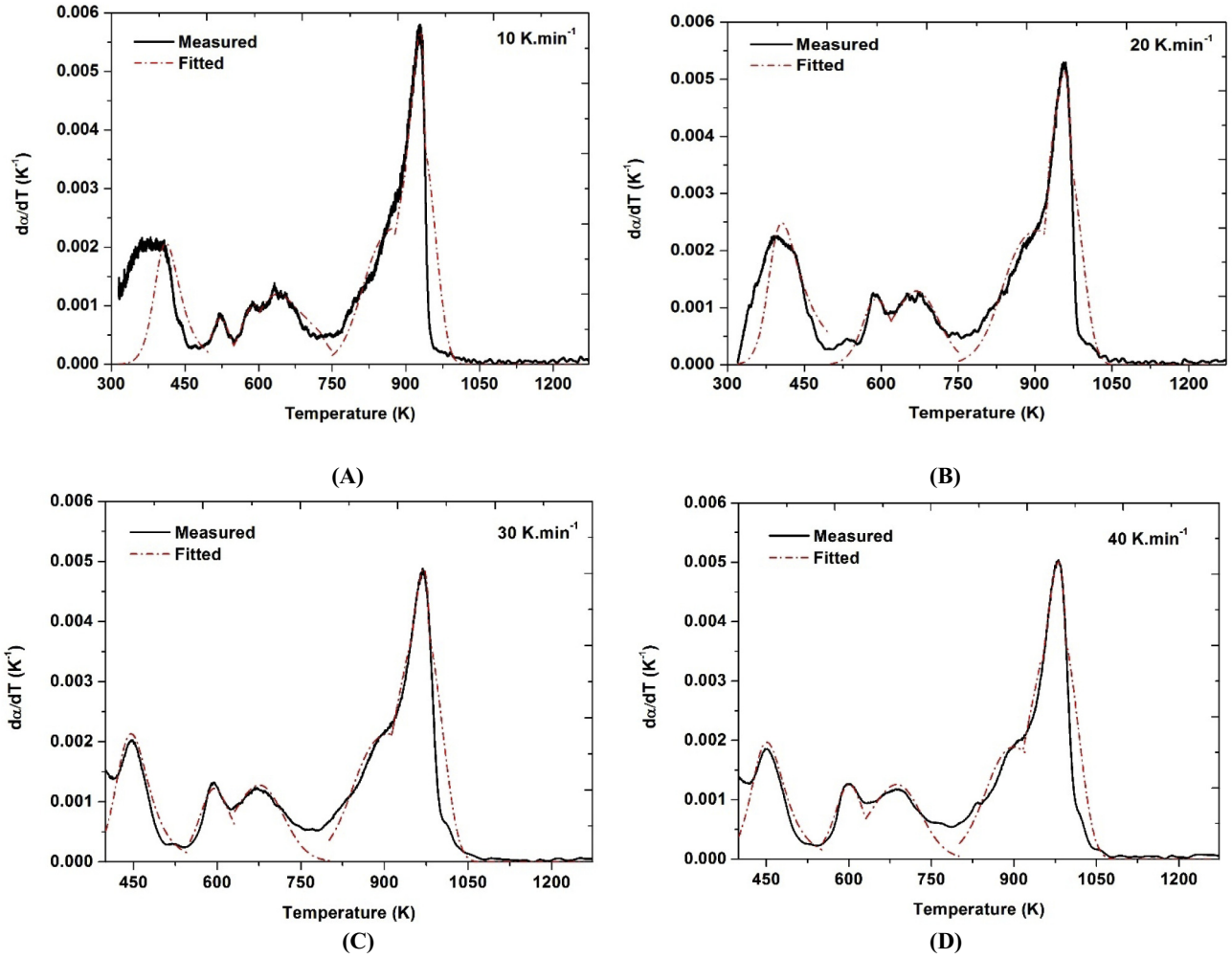

Fig. 7. Measured (solid line) and fitted (dashed line) TGA curves and deconvolution peaks for individual heating rates for 7C loaded with waste nitrates for different heating rates (A) 10 K.min^{-1}, (B) 20 K.min^{-1}, (C) 30 K.min^{-1} and (D) 40 K.min^{-1}.

References

[1] E. Vernaz, S. Gin, C. Veyer, Waste glass, in: R.J.M. Konings (Ed.), Comprehensive Nuclear Materials, Elsevier, Amsterdam, 2012, pp. 451–483.

[2] K. Raj, K.K. Prasad, N.K. Bansal, Radioactive waste management practices in India, Nucl. Eng. Des. 236 (2006) 914–930.

[3] B.K. Maji, H. Jena, R. Asuvathraman, Electrical conductivity and glass transition temperature (Tg) measurements on some selected glasses used for nuclear waste immobilization, J. Non-Cryst. Solids 434 (2016) 102–107.

[4] T. Okura, N. Yoshida, Immobilization of simulated high level nuclear wastes with Li_2O-CeO_2-Fe_2O_3-P_2O_5 glasses, Int. J. of Chem. and Molecular Eng. 6 (2012). No.8.

[5] R.F. Taylor, Chemical Engineering problems of radioactive waste fixation by Vitrification, Chem. Eng. Sci. 40 (No. 4) (1985) 541–569.

[6] K. Kawai, T. Fukuda, Y. Nakano, K. Takeshita, Thermal decomposition analysis of simulated high-level liquid waste in cold cap, Nucl. Sci. Technol. 2 (2016) 44, 1-7.

[7] H.N. Guerrero, D.F. Bickford, H.N. Neshat, Numerical models of waste glass Melters Part II - Computational modelling of DWPF, in: Proceedings Westinghouse Savannah River Co, 2003, pp. 1–10. WSRC-MS-2003-00272 Part II.

[8] R. Pokorný, D.A. Pierce, P. Hrma, Melting of glass batch: model for multiple overlapping gas-evolving reactions, Thermochim. Acta 541 (2012) 8–14.

[9] C. Rodriguez, J. Chun, D. Pierce, M. Schweiger, P. Hrma, Kinetics of cold cap reactions for vitrification of nuclear waste glass based on simultaneous differential scanning calorimetry -thermogravimetry (DSC - TGA) and evolved gas analysis (EGA), in: Proceedings of W M Conference, 2014.

[10] R. Pokorny, J.H. Zachary, D.R. Dixon, M.J. Schweiger, D.P. Guillen, A.A. Kruger, P. Hrma, One-dimensional cold cap model for melters with bubblers, J. Am. Ceram. Soc. 98 (2015) 3112–3118.

[11] S. Lee, P. Hrma, R. Pokorny, J. Klozek, V. Vander, D.R. Dixon, S.A. Luksic, Rodriguez, C.P. Chun, J. Schweiger, M.J. Kruger, A. Albert, Effect of Melter feed foaming on the heat flux to the cold cap, J. Nucl. Mater. 496 (2017) 54–65.

[12] G. Suneel, P.M. Satya Sai, C.P. Kaushik, J.K. Gayen, K.V. Ravi, Amitava Roy, Experimental investigations and numerical modelling of Joule Heated Ceramic Melter for vitrification of radioactive waste, Journal of Hazardous, Toxic and radioactive waste 23 (2019) 1–14.

[13] H.E. Kissinger, Reaction kinetics in differential thermal analysis, Anal. Chem. 29 (1957) 204–237.

[14] E.S. Freeman, B. Carroll, The application of thermoanalytical techniques to the reaction kinetics: the thermogravimetric evaluation of the kinetics of the decomposition of calcium oxalate monohydrate, J. Phys. Chem. 62 (1958) 394–397.

[15] S. Vyazovkin, Modification of the integral isoconversional method to account for variation in activation energy, J. Comput. Chem. 22 (2001) 178–183.

[16] S. Vyazovkin, A.K. Burnham, J.M. Criado, L.A. Perez- Maqueda, C. Popescu, N. Sbirrazzuoli, ICTAC Kinetics Committee recommendations for performing kinetic computations on thermal analysis of data, Thermochim. Acta 520 (2011) 1–19.

[17] T. Liavitskaya, S. Vyazovkin, Delving into kinetics of reversible thermal decomposition of solids measured on heating and cooling, J. Phys. Chem. C 121 (2017) 15392–15401.

[18] P.K. Mishra, D. Vaishali, D.E. Ghongane, T.P. Valsala, M.S. Sonavane, Preparation and Characterisation of Glass product with modified composition for Vitrification of high level radioactive waste, J. Therm. Anal. Calorim. 112 (2013) 103–108.

[19] D. Banerjee, V.K. Sudrasan, A.J. Joseph, R.K. Mishra, I. Singh, P.K. Wattal, D. Das, Role of TiO2 on physicochemical properties of cesium borosilicate glasses, J. Am. Ceram. Soc. 93 (2010) 3252–3258.

[20] M.I. Ojovan, W.E. Lee, C. Veyer, in: An Introduction to Nuclear Waste Immobilisation, second ed., Elsevier, Waltham, 2014.